NGST fine guidance sensor

N. Rowlands[a], J. Hutchings[b], R. Murowinski[†b], R. Alexander[‡c]
[a]EMS Technologies; [b]Herzberg Institute of Astrophysics; [c]Canadian Space Agency

ABSTRACT

Instrumentation for the Next Generation Space Telescope (NGST) is currently in the Phase A definition stage. We have developed a concept for the NGST Fine Guidance Sensor or FGS. The FGS is a detector array based imager which resides in the NGST focal plane. We report here on tradeoff studies aimed at defining an overall configuration of the FGS that will meet the performance and interface requirements. A key performance requirement is a noise equivalent angle of 3 milli-arcseconds to be achieved with 95% probability for any pointing of the observatory in the celestial sphere. A key interface requirement is compatibility with the architecture of the Integrated Science Instrument Module (ISIM).

The concept developed consists of two independent and redundant FGS modules, each with a 4' x 2' field of view covered by two 2048 x 2048 infrared detector arrays, providing 60 milli-arcsecond sampling. Performance modeling supporting the choice of this architecture and the trade space considered is presented. Each module has a set of readout electronics that perform star detection, pixel-by-pixel correction, and in fine guiding mode, centroid calculation. These readout electronics communicate with the ISIM Command & Data Handling Units where the FGS control software is based. Rationale for this choice of architecture is also presented.

Keywords: Next Generation Space Telescope; infrared imaging; guidance sensor; star tracker; astronomical instrumentation

1. INTRODUCTION

The Next Generation Space Telescope is a large diameter (6 m class) infrared optimized telescope to be placed at the L2 Lagrangian point ~1.5 x 10^6 km from the earth. In this low background environment, NGST will be orders of magnitude more sensitive than any ground based telescope in the 1 to 5 μm wavelength region. With this increased sensitivity NGST is expected to probe the early universe in unprecedented detail. Routine photometric and spectroscopic observations of objects with redshifts (z) greater than 10 will be possible, whereas $z \sim 5$ is at the observational limit of the Hubble Space Telescope.

A design reference mission has been produced [*cf* 1] which outlines the science requirements of the mission. Further refinement of these science goals and study of possible instrument configurations, led the Ad-Hoc Science Working Group (ASWG) to propose the following as the main instrument complement[2]:

1) A camera with near infrared and visible filters, sensitive over 0.6 – 5 μm
2) A multi-object dispersive spectrograph (MOS) for 1 – 5 μm, with R~1000
3) A combined camera / slit spectrograph for 5 – 28 μm with R~1500

These instruments are described in more detail in other papers within these proceedings.

[] rowlands.n@emstechnologies.ca; phone (613) 727-1771; fax (613) 727-9640; http://www.ems-t.com; EMS Technologies Canada Ltd., 1725 Woodward Drive, Ottawa, Ontario, Canada, K2C 0P9
[] john.hutchings@hia.nrc.ca; phone (250) 363-0018; fax (250) 363-0045; Herzberg Institute of Astrophysics, National Research Council of Canada, 5071 West Saanich Road, Victoria BC V8X 4M6
[†] richard.murowinski@hia.nrc.ca; phone (250) 363-0057; fax (250) 363-0045; http://www.hia.nrc.ca; HIA
[‡] russ.alexander@space.gc.ca; phone (613) 990-0807; fax (613) 952-0970; http://www.space.gc.ca; Space Science Program, Canadian Space Agency, PO Box 7275, Ottawa ON K1L 8E3

Before April 2001, the Near-Infrared Camera (NIRCam) instrument (item 1 above) also had the additional requirements of providing the facility services of guiding and wavefront sensing and control (WFS&C). After initial commissioning of the observatory, the WFS&C and control function will be infrequently performed (on the order of once a week). However, guiding is a real-time function that is contemporaneous with the science observations. The guiding function provides a continuous measurement of the line-of-sight direction, which in turn is used in a control loop to stabilize this line-of-sight at the Observatory level. After April 2001, this functionality was dropped from the NIRCam because it was determined that this real time function would result in some reduction in the efficiency of science observations. The guiding functionality now resides in a dedicated Fine Guidance Sensor (FGS). An instrument concept for the NGST Fine Guidance Sensor is the subject of this paper.

2. FGS REQUIREMENTS

Draft FGS requirements have been established by the NGST Project and are shown in Table 1. The relevant Observatory requirement which is applicable to the FGS states: "the Observatory shall have greater than 95% probability of acquiring a guide star and maintaining pointing stability for any valid pointing direction"[3]. The other key requirements are the update rate and noise equivalent angle[1]. These, along with the 95% requirement and the expected stellar density, set the field of view requirement for the FGS. The budget of 3 milli-arcseconds (mas) for the FGS contribution to the line-of-sight stability requirement is preliminary. The Observatory level requirement is 5 mas.

Table 1 Preliminary Fine Guidance Sensor Requirements

Parameter	*Value*
Guide Star Availability	> 95% probability for any pointing
Update Rate	20 Hz
Fine Guiding NEA	< 3 mas

An extensive sampling of the tradeoff space of the FGS system level parameters was performed in order to assess the appropriate field of view and PSF required for the FGS. Some of this tradeoff space and the resulting performance is described in Sections 3 & 4.

In addition to the above requirements, which define the FGS performance in fine guiding mode, the FGS must locate the guide star and initiate fine guiding within the range of the Observatory pointing control uncertainty. This control uncertainty is expected to consist of 5" (1σ radial) attitude knowledge error with a 3000s time constant superimposed on an attitude error of 1" RMS over a uniform frequency spectrum of 0 to 0.02 Hz. Section 5.0 discusses the implications of these pointing errors on the acquisition and identification processes.

In order to meet the fault tolerance requirement of no single failure causing *any* degradation in performance [3], we propose that two independent FGS modules be required. The intent is to only use one module at any given time, with the second as a cold standby. This may be re-visited if there are preferred locations in the NGST field of view for the FGS modules with respect to the science instruments.

[1] For the purposes of this document Noise Equivalent Angle is defined as the RMS (1σ) standard deviation of centroids calculated in a Monte-Carlo simulation of the sampled stellar images with added noise.

3. FINE GUIDING PERFORMANCE

A numerical simulation of the noise equivalent angle (NEA) was developed in order to evaluate the sensitivity of the FGS fine guiding performance to many of the instrument parameters. The model begins with a point-spread simulation. In support of general NGST studies, a prescription for a "Reference Telescope" was developed at NASA Goddard in support of instrumentation studies. This design is similar to the designs proposed for the Optical Telescope Element (OTE) by the potential prime contractors. The Reference Telescope has a physical diameter of 6m, an effective area of 25 m^2 and an f-number of f/20. The PSF was simulated using the Huygens diffraction calculation within the optical raytrace code ZEMAX. Low and mid-scale spatial frequency aberrations were added to the primary mirror in order to simulate an optical quality that just meets the NGST OTE requirement of diffraction limited (Strehl = 0.8) at 2 μm and an encircled energy of 75% in 150 milli-arcseconds [3].

A number of monochromatic PSF's were finely sampled (in 6 milli-arcsecond bins) and from this data set, polychromatic PSF's were synthesized for different wavelength weightings, thus simulating different stellar spectral energy distributions. Analyses of star count statistics show that at the magnitude range of interest for the FGS; by far the most common stellar spectral type is M0 [5,6]. We adopted this spectral type for all the FGS the modeling presented here. Except for very early spectral types, there is little variation in the results as a function of stellar type or metallicity.

Table 2 summarizes the assumptions used in the modeling. The detector performance listed is derived from the NGST requirement of 10 electrons readout noise for the focal plane system [4]. The FGS will likely make use of the detectors arrays being developed for the NGST NIRCam and NIRSpec instruments. There currently are two 2048 x 2048 format focal plane arrays (FPAs) under development: InSb with 25 μm pixels and 5 μm cutoff HgCdTe with 18 μm pixels. Our current assessment of both detector types is that either are suitable for the FGS application, assuming they meet the NGST requirement. The FGS requires fast readout of a small (4x4) window around the selected guide star. Again our current assessment of both detector multiplexers under development for NGST is that either will support the required windowed frame rates. There is expected to be some readout overhead in the operation of the detectors so that for the modeling purposes it is assumed that 40 ms of integration time is available using a readout consisting of 4 Fowler sample pairs.

Table 2 FGS NEA Modeling Assumptions

Parameter	Value
Stellar Type	M0 (solar metallicity)
Telescope Diameter	6.5 m
Telescope Effective Area	25 m^2 (25% obscuration)
Telescope & FGS Throughput	63% [1]
Detector Quantum Efficiency	80%
Detector Readout Noise	14 e- [2]
Effective Integration Time	40 ms
Wavelength Ranges	0.8 to 2.5 μm, 0.6 to 3.0 μm, & 0.6 to 5.0 μm
Window Size	4 x 4 pixels
Centroiding Algorithm	"FFT"[3]

Notes to Table 2:
1) Assumes 95% end-of-life reflectance per surface & 9 surfaces total to the FGS detectors
2) The readout noise has been scaled from 8 Fowler sample pairs as assumed in [4] to 4 Fowler sampling
3) The centroiding technique is based on a fast fourier transform of the row & column sums of the small readout window [7].

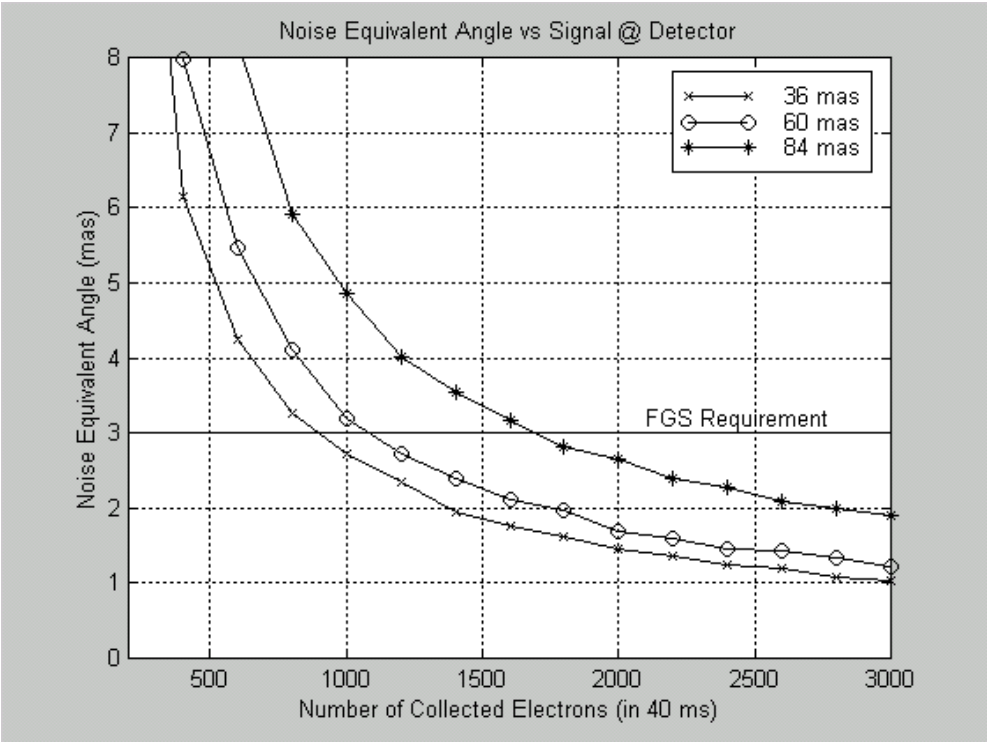

Fig. 1 Noise Equivalent Angle verses signal in electrons at the detector for three different angular samplings of the PSF (pixel size). The wavelength range is 0.8 to 2.5 μm.

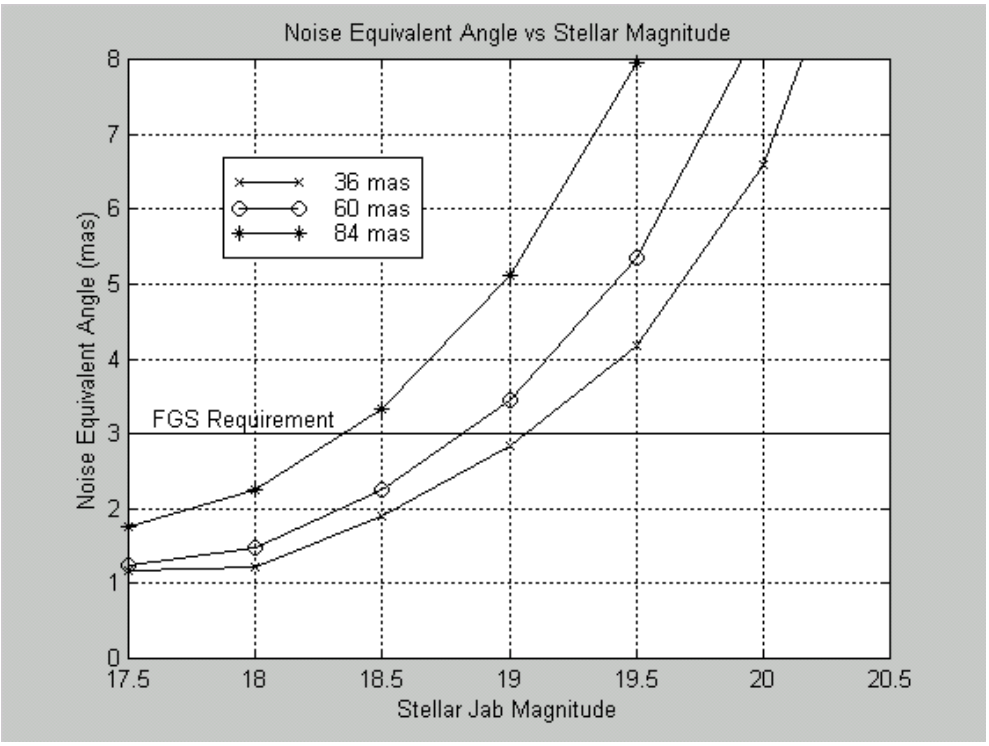

Fig. 2 Noise Equivalent Angle verses stellar magnitude for three different angular samplings of the PSF (pixel size). The wavelength range is 0.8 to 2.5 μm.

Figure 1 shows the Noise Equivalent Angle as a function of collected signal in electrons on the detector, while Figure 2 shows the NEA as a function of stellar magnitude. From these results it can be seen that the FGS performance of 3 mas can be obtained for stars brighter than Jab=18.8 magnitude in the case of 60 milli-arcsecond sampling of the PSF. For comparison, this equates to J=17.9 and K=17.1 for an M0 spectral type.

Different wavelength ranges (and hence different PSF sizes) were also modeled. There were small increases in NEA as the PSF size increased given the same collected signal in electrons at the detector. The polychromatic PSF shape for an M0 star is dominated by the 0.8 to 2.5 μm wavelength region. There is however, slightly more light available in the broader wavelength ranges even with the heavy weighting to the 0.8 – 2.5 μm region due to the M0 spectral energy distribution. Figure 3 shows the combination of these two effects in a plot of NEA vs stellar magnitude for the 0.8 to 2.5 μm, 0.6 to 3.0 μm and 0.6 to 5.0 μm wavelength regions and for a fixed pixel sampling of 60 milli-arcseconds. In terms of the limiting magnitude for the required 3 milli-arcseond NEA, expanding the 0.8 to 2.5 μm wavelength range to 0.6 to 3.0 μm increases the FGS sensitivity by ~0.1 magnitudes while expanding to 0.6 to 5.0 μm provides a further sensitivity increase of ~0.1 magnitudes.

There is a potential testing advantage if the wavelength range is limited to shorter wavelengths since the overall instrument would not need to be cooled to the ISIM operating temperature for all tests. The detector and its housing (which might include a long wavelength cutoff filter if an InSb FPA or a 5 μm cutoff HgCdTe FPA is employed) would still need to be cooled to close to the ISIM operating temperature of ~30K to 35K. The baseline choice is thus the more restricted wavelength range.

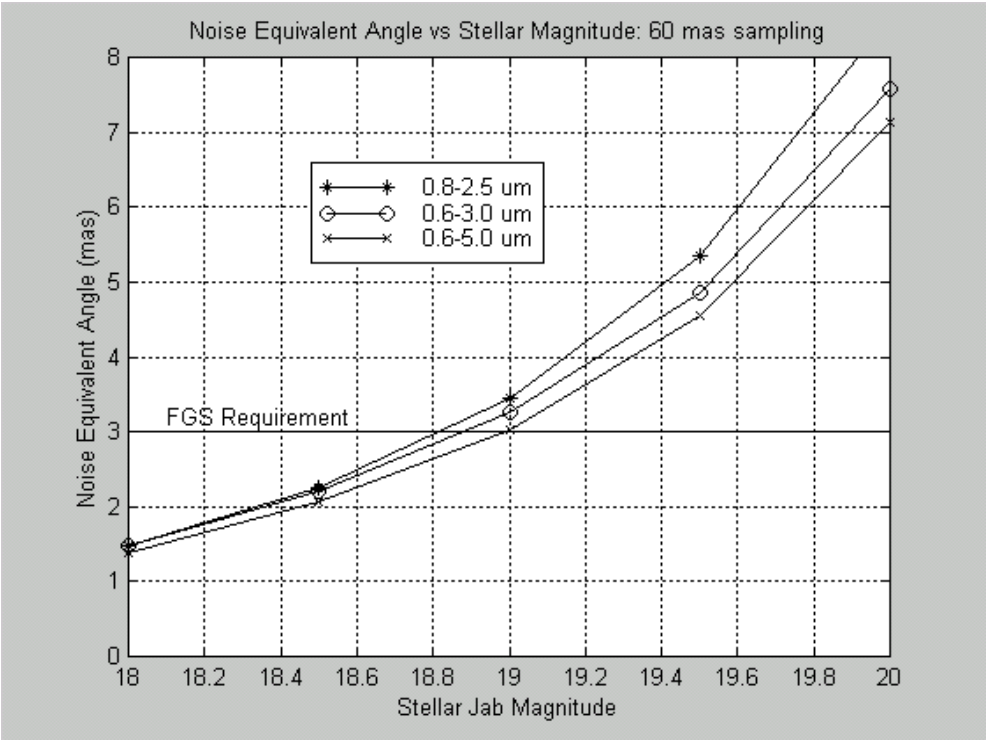

Fig. 3 Noise Equivalent Angle verses stellar magnitude for three different wavelength ranges. The PSF sampling is fixed at 60 milli-arcseconds per pixel.

The NEA performance has also been modeled as a function of various instrumental effects such as instrument focus and optical alignment. These analyses suggest some margin on the performance should be taken to allow for degradations in performance due to effects like the build up of optical alignment budgets. If we conservatively plan for an NEA of ~2 milli-arcseconds in the absence of these effects, then it can be seen from Figure 2 that this is equivalent to a decrease in limiting magnitude of ~0.5 magnitudes. For example at 60 milli-arcsecond sampling the limiting magnitude would then be Jab = 18.3. This limiting magnitude is used in the next section to illustrate the choice of the FGS field of view and the overall architecture of the instrument. A more complete NEA budget from all sources will be developed in the next phase of the project.

4. ARCHITECTURE TRADEOFF

A trade study was undertaken to determine the optimum architecture of the NGST Fine Guidance Sensor. The main issue is the field of view that must be accessible to the FGS in order to find stars which are bright enough for the fast guiding operation. Options considered fell into three general categories:

1) Small area detector arrays fed by actuated optics positioned across a wide field of view.
2) Large area detector arrays in the NGST OTE focal plane
3) Re-imaging optics and moderately sized area detector arrays to optimize the sampling of the PSF

Option 1 was rejected for three reasons. First it was felt that the reliability and travel required of the cryogenic mechanisms would be incompatible with the FGS requirements. Second, the FGS is part of the control loop for the line of sight stabilization system. With an actuated FGS, the control loop for the FOV positioner is then imbedded within a larger control loop and this was seen as a significant complicating factor. Third, the requirement for large travel dithers between science images (up to 20") and a potential requirement for tracking are both best served by an FGS with a large monolithic field of view.

While Option 2 is attractive from the point of view of simplicity, a significant reduction in the number of detector elements is possible if re-imaging optics are employed to provide coarser sampling of the PSF. In the modeling described in Section 3.0 it was assumed that some form of relay optics are used to allow the PSF to be sampled at the various intervals (36, 60 and 84 mas are shown in the plots).

Figure 4 shows the tradeoff in terms of PSF sampling (angular size of the pixels in the NGST OTE focal plane) and number of pixels required to cover the field of view. The field of view is set by the requirement that on average 3 stars of sufficient brightness are present when the Observatory is pointed to the most sparsely populated region of the sky. This gives the 95% probability of finding a suitable guide star in any portion or the sky. There are different expectations for stellar counts in the range of the NGST FGS sensitivity [5,6]. For the calculations used to obtain the field of view requirements shown in Figure 4, both the modeled [5] and observed [6] stellar counts were used.

Figure 4 provides a means of estimating the number of pixels required for Option 2 with FGS detector arrays placed directly in the NGST Reference Telescope focal plane. The PSF sampling would be either ~40 mas for 25 μm pixels or ~30 mas for 18 μm pixels. For the model star count case, either 4400^2 or 5300^2 pixels would be required for 25 μm and 18 μm pixels respectively. In terms of equivalent number of 2k x 2k focal plane arrays, this equates to 4.6 or 6.7 focal plane arrays for the 25 μm and 18 μm pixels respectively.

Placing a large number of Focal Plane Arrays directly in the NGST focal plane, has an impact on the packaging of the FGS with the Science Instruments. For Option 2 it is not just a matter of accommodating the imaging areas of the detectors, but also their fan out boards and connectors. These dead zones around the FGS detectors would take up substantial fraction of the NGST field of view and would seriously constrain the FGS placement with respect to the other instruments. While Option 3 would require a similar field of view size, the re-sampling reduces the number of pixels required and facilitates packaging as extra space around the FGS field-of-view in the NGST focal plane is not required.

For the reasons of cost and anticipated packaging issues Option 3 was selected as the most viable architecture for the FGS instead of Option 2. The pixel sampling and field of view chosen for study as Option 3 was 60mas sampling with a 4k x 2k detector array for a field of view of 8.4 sq. arc min. This choice satisfies the FGS requirements even if the modeled star counts [5] are adopted. This choice includes margin as described in section 3.0. Also it is based on a conservative assumption for telescope throughput, and the assumption that the detectors just meet the NGST requirements.

Less pixels for the FGS are also possible, if the sampling size is increased. However, the overall field of view required increases with coarser sampling and this must be traded off against ISIM packaging issues. Optical designs that provide the required re-imaging performance have been investigated for the baseline 60 mas sampling and for sampling in the range of 50 to 80 mas per pixel.

Given that the FGS requires an optical relay system, the optical design could produce a point spread function that is different from the diffraction limited PSF (at 2 μm) in the NGST focal plane. However, the NEA simulations showed that the principally diffraction limited NGST PSF, sampled at 60 mas, provides sufficient "blurring" for accurate centroids to be obtained. Note that the FGS imaging performance is defined only in terms of the NEA. A wavefront error larger than that allocated for science imaging can be accommodated within the FGS.

Note that with the current FGS concept field of view, there is no existing stellar catalog with the requisite lower limiting magnitude from which to draw identification and guide stars in the region of the Galactic Poles. For the purposes of the FGS conceptual design it has been assumed that the nominal FGS field of view around the science target is known and the locations and approximate magnitudes of stars to be used for identification, acquisition and guiding are provided to the FGS before the identification process begins.

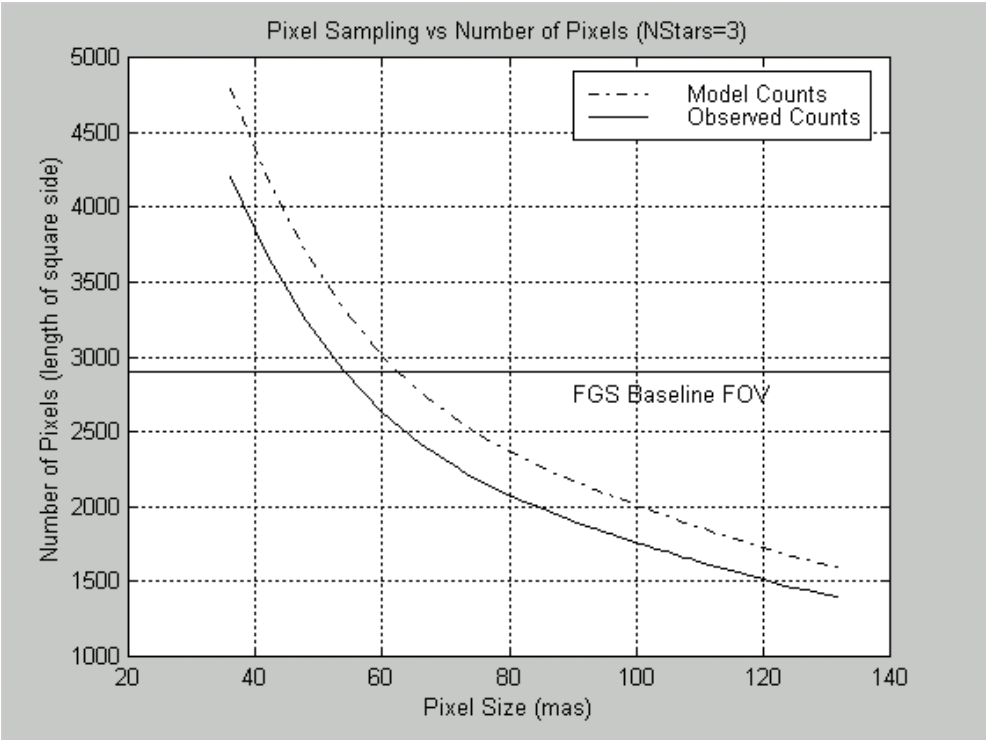

Fig. 4. Number of Pixels in the FGS field of view versus the sampling size for 95% guide star probability at the North Galactic Pole. The curves represent different stellar densities as described in the text and in [5] & [6]. The "FGS Baseline Field of View" line in the figure is equivalent to a field of view sampled with 4k x 2k detectors. With 60 mas per pixel this corresponds to our baseline FGS concept design FOV of 8.4 square arc minutes. The 95% probability is met when there are, on average three stars present in the FOV.

5. BASELINE CONCEPT DESIGN

1. Block Diagram

The major functional and physical blocks of the FGS are shown in Figure 5. There are two functionally redundant Fine Guidance Sensors, either of which is capable of fulfilling the requirements. The two FGS assemblies are physically located within the Integrated Science Instrument Module (ISIM) and have optical, mechanical, thermal, electrical and software interfaces to the shared systems within the ISIM. The FGS processor in the current baseline is a software suite hosted by the ISIM Command and Data Handling (C&DH) Unit. There are two redundant ISIM C&DH Units that are cross-strapped to the Readout & Control Electronics of the two FGS assemblies, so that either C&DH Unit can operate either FGS Electronics.

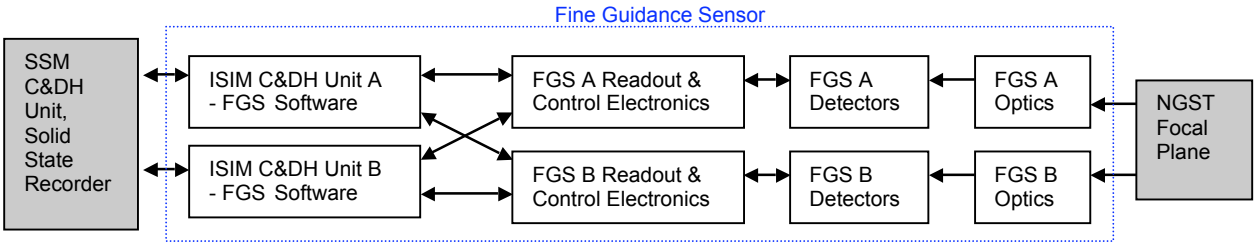

Fig. 5 Major Components of the Fine Guidance Sensor Sub-System and the interfaces to the ISIM Element and Spacecraft Element Sub-Systems (SSM is the Spacecraft Support Module).

The four components can be described as follows:

- Optics: including structure, optical elements & thermal control. The optics relay the FGS field of view to the FGS detectors
- Detectors: two 2kx2k FPA's assembled into a Sensor Chip Assembly (SCA), pre-amplifier circuit & harness. The detectors sample the PSF and provide an analog signal proportional to the incident light.
- Readout & Control Electronics: including detector control, windowed image processing, instrument health monitors, power conditioning and communications interfaces. The Electronics select and clock out regions within the SCA's, and provide pixel-by-pixel correction and small window centroiding.
- FGS Software: guider executive with interface to the Observatory Program Executive (the supervisory software or OPE), full image processing & image recognition, communications with & control of FGS Readout & Control Electronics. The FGS software is resident in the ISIM C&DH Unit.

2. Functional Modes & Description

The principal operating functions of the FGS are:

a) Identification: Recognizing the star pattern in the FGS field of view so that the guide star may be identified
b) Acquisition: Using the identified guide star to provide coarse line-of-sight monitoring at low update rate to the fine steering mirror controller so that initial line-of-sight stability is obtained.
c) Fine Guiding: Using the identified guide star provide line-of-sight monitoring at the required rate and precision for nominal science operations.

These functions are implemented partly by software and partly by hardware. This functional split is described in more detail in Section 5.4.

In identification the following steps will be followed:

1) The FGS Software receives a command to begin identification and commands the FGS Readout Electronics to acquire a full correlated double sampled (CDS) image with 1-2s integration time using a ripple mode readout. In this mode a subset of each FPA (256 x 2048) is read out with 1-2s between samples. These sub-images are passed to the FGS Software in the ISIM C&DH Unit for

assembly into a complete image. Longer integrations are not required (or needed) due to the telescope motion: 1" (1□) over 0-0.02 Hz + 5" (1□) drift over 3000s.

2) Identified stars in the identification image are compared to an uploaded table of stellar locations in the guide field by FGS Software
3) If a match is made, the FGS Readout & Control Electronics are then commanded to acquire window images centered on the location of the identified stars. This allows the drifting stellar field to be imaged quickly (within ~1s).
4) Field identification is confirmed and the guide star location in the FGS field of view determined.
5) Note that a pre-determined number of stars (~10, TBC) will be needed for identification. In order to minimize the number of stars being processing for the matching algorithm, the magnitude range of these identification stars would depend on the galactic latitude. This range is likely to be: 14 < Jab < 21. The integration times and thresholds for the identification process will be determined by this magnitude range.

The steps during acquisition are:

1) The FGS Software commands the FGS Readout & Control Electronics to acquire a large windowed CDS image (up to 256 x 256 pixels in size) around the guide star using a long integration time (~1 s).
2) The FGS Software calculates a centroid for the guide star and passes this information to the Spacecraft Control Module Command & Data Handling Unit (via the ISIM C&DH Unit) so that Line-of-Sight stabilization can commence
3) Windowed images and centroids are continuously produced with the window becoming successively smaller, giving a corresponding increase in the centroid update rate. Note that a transition star may be required in the early acquisition steps if, for example the chosen guide star is close to another object. At a predetermined (small) window size a transition would be made to the chosen guide star. A transition star can be dimmer than guide star due to the lower update rates.
4) At 8x8 window size the FGS autonomously enters Fine Guiding.

The steps during Fine Guiding are:

1) Window image size becomes 4x4 and Fowler 4 sampling is initiated for optimum readout noise
2) Update rate fixed at guide rate (20 Hz TBC)
3) Small scale (<1") dithers are likely possible in Fine Guiding Mode as it can be implemented with small motions of the fine steering mirror.
4) Large scale (up to 20") dithers may be possible if the direction of the dither is planned (to keep the guide star in the field of view) and if the coordinated motion of the fine steering mirror and body pointing of the Observatory is sufficiently uniform.
5) Tracking may be possible in Fine Guiding Mode as long as the motion does not cross an FPA boundary or defect. Although not part of the formal FGS requirements, a tracking rate of < 0.015 arc-seconds / second appears to be a feasible requirement.

3. Opto-Mechanical Design

Figure 6 shows a solid model representation of one of the opto-mechanical designs being considered for the FGS Optics Module. The optics consists of a pickoff mirror, three curved mirrors (2 spherical & 1 conic), a fold mirror and the detector mounting. No filters (or filter wheel) are expected to be required, except possibly a fixed band-limiting filter at the detector. The FGS imaging performance is not as strict as that for the other science instruments and the PSF should be coarsely sampled (Section 4.0). In addition to any of the NGST OTE wavefront errors, the FGS wavefront error budget will likely be on the order of ~100 nm. A preliminary tolerance budget has been developed based on this system allocation.

The fold mirror indicated in Figure 6 could also serve as a focus control if required. Preliminary NEA budgeting seems to indicate that the allocated ±2 mm of focus change at the focal plane can be accommodated so that a focus mechanism may not be required. This conclusion, and the optical performance budgets will be revised as the overall NGST designs evolve. The pickoff mirror shown can be oriented differently or removed entirely depending on the packaging arrangement chosen.

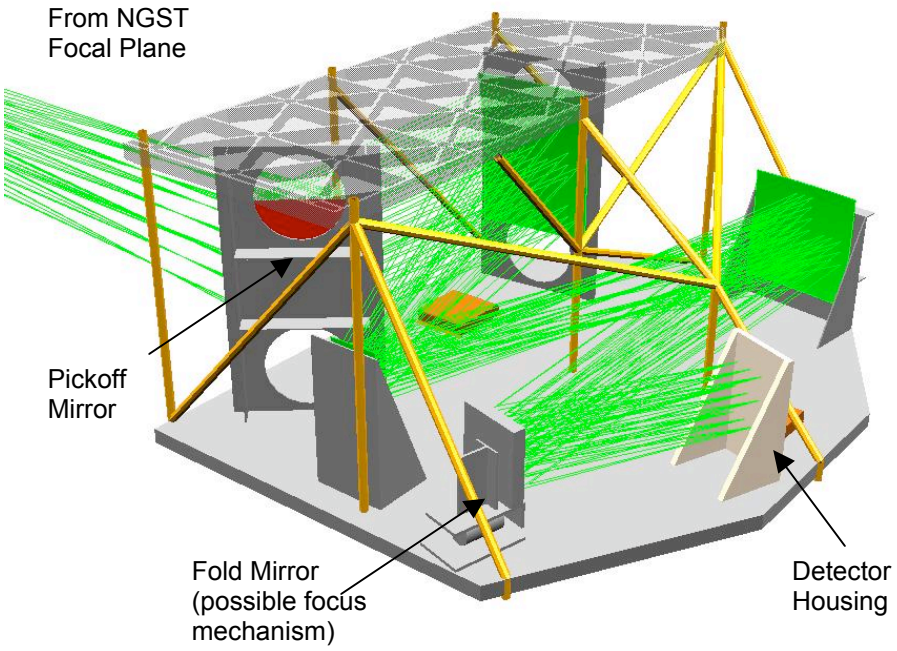

Fig. 6 Opto-mechanical layout of one possible FGS design. This design gives 60 mas sampling with 18 μm pixels using the Reference Telescope, designs for different samplings and 25 μm pixels have been developed and are similar to this example. Rays outlining the FGS field of view are shown transiting the instrument. This plane & strut design makes use of AlBeMet as the structural material and for the optical elements themselves. The volume is ~ 0.75 m^3 (490 x 850 x 1040 mm) and the mass is estimated as ~25kg.

4. Electronics Architecture

Figure 7 shows a block diagram of the FGS Readout & Control Electronics and the current concept for interconnection with the ISIM Command & Data Handling Units. Each set of FGS Readout & Control Electronics must control two Focal Plane Arrays each having 2048 x 2048 pixels. The FGS Readout & Control Electronics are structured so that the control and data paths from the two FPA's are handled separately. Thus over and above the redundancy of having two completely separate FGS modules, there is a graceful degradation path for each FGS module should one of its FPA's and/or one of the direct FPA control electronics fail.

The Readout & Control Electronics for each FGS module consists of six circuit card assemblies (CCA's) in an enclosure. There are two sets of FGS Electronics, one for each module. One FGS module is designated "FGS A" while the other is designated "FGS B". The six CCA's within each module are:

1) Focal Plane Array Sequencer / Timing CCA for FPA#1 (FPS#1)
2) Focal Plane Array Sequencer / Timing CCA for FPA#2 (FPS#2)
3) Detector Interface CCA (Analog-to-Digital Converter) for FPA#1 (DIF#1)
4) Detector Interface CCA (Analog-to-Digital Converter) for FPA#2 (DIF#2)
5) FGS Instrument Control Electronics CCA (ICE)
6) Power Distribution / Conditioning CCA (PDC)

There are an additional two CCA's, called the FPA Headboards, located adjacent to the Focal Plane Arrays within the cold Optics Component. These CCA's provide for cable termination and isolation.

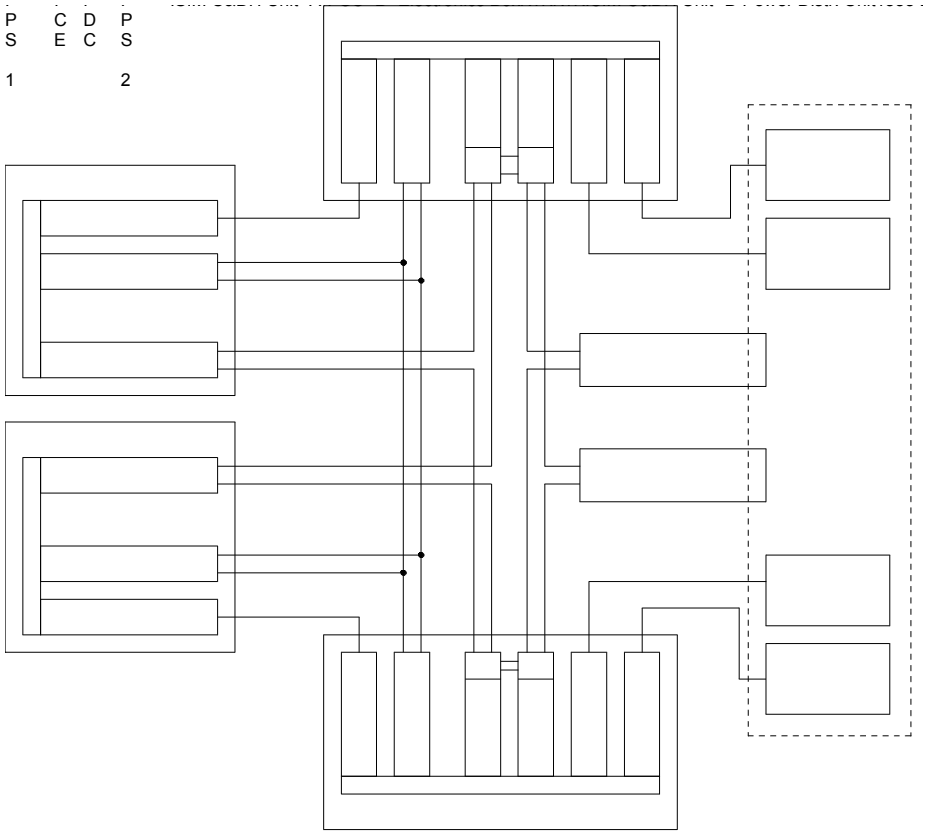

Fig. 7 Block Diagram of the FGS Readout & Control Electronics, including the interconnections with the ISIM data and command interfaces. The command bus is based on IEEE-1553 standards while the data bus is based on the IEEE-1355.2 (Spacewire) standard. "RTR" above refers to a 1355 router chipset.

The FGS Software resident in either of the ISIM C&DH Units (only one is operational at one time) commands the FGS Readout & Control Electronics via the redundant IEEE-1553 command bus to the Instrument Control Electronics (ICE) CCA. These commands are interpreted and passed to the Focal Plane Sequencer (FPS) CCA's, which in turn set up the detector clocking patterns and the Detector Interface (DIF) CCA for the commanded observation. Once the image data is readout by the FPS it is transferred to the FGS Software resident in the ISIM C&DH Unit across the IEEE-1355 interface that is common for all the image data from all the science instruments.

The Detector Interface CCA produces the bias levels required for each FPA, it hosts the analog chain which applies gain and offset to the analog FPA output and also applies the analog to digital conversion (16 bits). This data is passed to the FPS CCA over a parallel bus data bus. Since there are four FPA outputs there will be four parallel data paths to each FPS. The FPS provides buffer space for the image data and also applies pixel-by-pixel corrections such as offset correction. There is a large EEPROM bank on the FPS for this purpose. After the last sample is acquired for a given image, the FPS applies a cosmic ray rejection algorithm (if required), a star identification algorithm and if the latter is positive, a centroiding algorithm. A hardware implementation of the centroiding was felt to be the best way to achieve a minimal and deterministic data latency in fine guiding mode. Note that in the other modes the FGS software resident in the ISIM C&DH Unit performs the star identification and centroid calculations. In fine guiding mode the centroids are passed to the ISIM C&DH Unit across the, deterministic IEEE-1553 bus via the ICE CCA.

At some level there will be uncertainties in the telescope performance in areas such as straylight and exact PSF shape, it is therefore very desirable that the centroiding, star identification and pixel by pixel

correction algorithms all be programmable. In order to provide this programmability, each FPS will be implemented in either an Field Programmable Gate Array configuration with programmable EEPROM tables, or in an embedded Digital Signal Processor (DSP) implementation. Since the FPS is not required to store a full image, assuming the ripple mode readout is implemented in identification mode as described in Section 5.2, then only a limited amount of RAM, on the order of ~1 Mbyte, is required on each FPS CCA. This memory is sufficient to store the 256 x 2048 image slices required in the first step of identification mode and also the 8 256 x 256 windowed images as required during the confirmation portion of the identification phase.

There is one ICE CCA for each FGS Module. This board is independent of either of the two FPS + DIF + SCA strings and allows independent health & status monitoring of the FGS. The FGS Electronics also contains a Power Distribution & Conditioning (PDC) CCA. This CCA contains multiple sections for the different analog and digital voltages required by all the FGS electronics. It is assumed that the ISIM supplies unregulated power to the FGS Electronics.

6. CONCLUSIONS

We have described the current concept for the NGST Fine Guidance Sensor. The initial tradeoffs have led to an imager based FGS with a 4.1' x 2.05' field of view sampled at 60 milli-arcseconds per pixel. Performance modeling in fine guiding mode has assumed detectors that meet the NGST requirements and has used an aberrated Reference Telescope. The model results show that the baseline FGS will meet the overall NEA requirement of 3 milli-arcseconds at 20 Hz update rate for stars brighter than J_{ab}=18.3. This sensitivity estimate includes some margin. With this sensitivity limit the baseline FGS will meet the requirement of a >95% probability of obtaining a usable guide star for any telescope pointing. Preliminary opto-mechanical and electronics designs have been produced. These concept designs meet the interface requirements of the Integrated Science Instrument Module.

ACKNOWLEDGEMENTS

We would like to gratefully acknowledge the work of all the members of the Canadian FGS Concept Study team: Tim Hardy, Chris Morbey and Darren Erickson at HIA and, Brian Mackay, Shiguang Wang, Malcolm Moody, Julia Zhou, Lorne Yanosik, Joel Houde, and Andrew Bell at EMS Technologies. We would also like to acknowledge the assistance of the members of the ISIM Project Team at NASA Goddard Spaceflight Center. The FGS concept design work at EMS was performed under CSA contract number: 9F007-001114/001/SR.

REFERENCES

1. E.P. Smith, J.C. Mather, H.S. Stockman, P.Y. Bely, M. Stiavelli, R. Burg , 1998, "Next-Generation Space Telescope design reference mission", *Proceedings of SPIE 3356, Space Telescopes and Instruments V*, Editor(s): P.Y Bely, & J.B. Breckinridge
2. J. C. Mather, P. Jakobsen, S. Lilly, P. Stockman, 10 January 2000 , "NGST Science Instrument Recommendations" (Doc# 549 at http://ngst.gsfc.nasa.gov)
3. "NGST Level 2 Requirements", NGST-RQMT-000634, August 10, 2001 (available as: http://prod.nais.nasa.gov/eps/eps_data/097125-SOL-001-009.doc)
4. "Technology Development Requirements and Goals for the NGST Detectors", NGST-RQMT-000787, Draft Release 8, October 30, 2001. (Doc# 641at http://ngst.gsfc.nasa.gov)
5. A. Spagna, 9 May 2001, "Guide Star Requirements for NGST, Deep NIR Star counts and Guide Star Catalogs", STScI-NGST-R-0013B, Issue B. (Doc# 422 at: http://ngst.gsfc.nasa.gov)
6. J.B. Hutchings, P.B. Stetson, A. Robin, & T. Webb, 11 March 2002, "Faint Star Counts in the Near-infrared", submitted to *Publications of the Astronomical Society of the Pacific*. (astro-ph/0204284)
7. "Optical Acquisition & Tracking System", October 26, 1999, US Patent 5,973,310. See also: W. Lunscher, B. Gordon, 1998, "An Acquisition & Tracking Sensor for Optical Inter-satellite Communication", *Proceedings of the 10th Conference on Astronautics*, Canadian Aeronautics and Space Institute, p365.